JOURNAL OF OPTOELECTRONICS AND ADVANCED MATERIALS Vol. 9, No. 10, October 2007, p. 2996 - 3001

Invited Lecture

Bond constraint theory and EXAFS studies of local bonding structures of $Ge_2Sb_2Te_4$, $Ge_2Sb_2Te_5$, and $Ge_2Sb_2Te_7$

M. A. PAESLER, D. A. BAKER, G. LUCOVSKY, P. C. TAYLOR[a], J. S. WASHINGTON
Physics Department, North Carolina State University, Raleigh, NC 27695-8202, USA
[a]Physics Department, Colorado School of Mines, Golden, CO 80401-1887, USA

Bond constraint theory (BCT) and rigidity theory provide powerful frameworks for understanding the structure and properties of a-materials. In this paper, we discuss the foundations of BCT and rigidity theory with particular emphasis on chalcogenide compounds with atoms of varying coordination. Application of these theories to switching in a-chalcogenides holds the promise of finding the best composition suited for switching applications [1]. Recently a-chalcogenide switching has been applied successfully to programmable memory devices [2] as well as DVD technology where the quest for the discovery of better-suited materials continues. Thus, switching grants researchers today with an active arena of technological as well as fundamental study. Extended X-ray Absorption Fine Structure (EXAFS) spectroscopy [3] is an ideally suited technique to investigate the switching properties of these materials. We predict that films of amorphous $Ge_2Sb_2Te_4$, $Ge_2Sb_2Te_5$, and $Ge_2Sb_2Te_7$ exhibit differing bonding structures and bond statistics, which result in different electronic and optical properties.

(Received July 3, 2007; accepted October 1, 2007)

Keywords: Amorphous Ge-Sb-Te films, Bond constraint theory, EXAFS, Local bonding

1. Introduction

The switching mechanism of phase change materials is an active area of study among researchers today. Phase change materials, such as $Ge_2Sb_2Te_5$ and $GeSb_4Te_7$, are very important to current applications such as DVD memory, and will form the basis of many future devices (PRAM, reconfigurable interconnects, etc.) [2]. These applications rely on the property changes associated with an amorphous-crystalline transition, however a description of this transition is an area of contention [4,9]. Using Extended X-ray Absorption Fine Structure (EXAFS) spectroscopy, we have examined and presented the results of the bonding structures and bond statistics of as-deposited films of $Ge_2Sb_2Te_5$. Interpretation of these results using the framework of bond constraint theory (BCT) [5, 6, 7, 8] demonstrates the suitability of each composition as a good glass former. We also present findings outlining the possibility that the change in overcoordinated Te between $Ge_2Sb_2Te_4$ and $Ge_2Sb_2Te_7$ may be significant to the amorphous-crystalline transition.

2. Experimental results

EXAFS measurements of as-deposited amorphous $Ge_2Sb_2Te_5$ (a-225) samples and the subsequent initial analysis are described elsewhere [9]. Table 1 presents a summary of (N) and nearest neighbor distances for the four atom pairs in a-225, while Fig. 1 and Fig. 2 show normalized absorption spectra and k^3-weighted EXAFS spectra, for all three edges, respectively. Nearest neighbor (N) determinations indicate fully coordinated Ge and Sb with N_{Ge} = 3.9±0.8 and N_{Sb} = 2.8±0.5 and slightly over coordinated Te with N_{Te} = 2.4±0.6. Note that the reported bond lengths of Te agree with tabulated covalent radii for each species [10]. The results are shown to be internally consistent for several reasons. First, the Te nearest neighbor distances $R_{Te\text{-}Sb}$ = 2.83Å and $R_{Te\text{-}Ge}$ = 2.62 Å) are found to be the same, within the error, regardless of whether they were determined from Te-edge data or from the neighboring atom data (Sb and Ge respectively). Second, neither the Ge data nor the Sb data indicate the presence of Sb–Ge bonding.

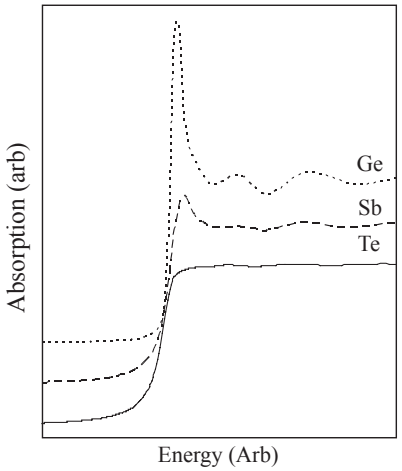

Fig. 1. Absorption spectra for all three atomic species, shifted in energy for comparison.

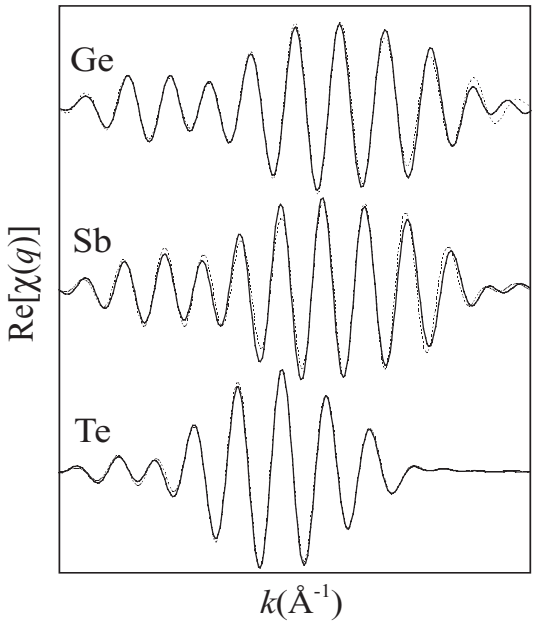

Fig. 2. Plots of k^3-weighted normalized EXAFS spectra for a-225. Solid lines are data, dashed lines are fits.

3. Discussion

In previous proceedings [11], we have discussed the bonding behaviour of Ge, Sb, and Te in the a-225 system; particularly, we looked at the preponderance of Ge-Ge bonds, and provided an explanation of the observed shortened Sb-Te bond. We saw from the EXAFS that every Ge in a-225 was likely bonded to another Ge and three Te, and that Ge–Ge bonds were the only like atom bonds which occurred.

In an analysis of the Ge-Te system, deNeufville refers to a $Ge_{17}Te_{83}$ glass which "closely idealized a metastable structure" [11]. This glass is found on the eutectic where glass transition temperature is lowest and phase change most likely to occur. In our $Ge_xSb_yTe_{1-x-y}$ system, one can hypothesize a composition which closely resembles this, namely $Ge_{17}Te_{83}$. In $Ge_{17}Te_{83}$, a Ge atom is bonded to four Te (see Fig. 3b) atoms with added Te–Te bonding allowed – an occurrence which will change our previous BCT calculations.

Given the molecular species in Fig. 3, of the possible Ge bonds, 1/11 (~9%) are homopolar Ge–Ge bonds. Although this result agrees within error with the EXAFS, our findings suggest that there are closer to 15% Ge–Ge bonds in 225. This implies that the Ge_2Te_3 configuration occurs more often than the $Ge_{17}Te_{83}$.

Evidence for Te–Te bonds in the 225 system is not reflected in the EXAFS. Because Sb and Te have difference in Z of only 1, it is very difficult to distinguish between bonds that include these atoms. Thus, a fraction of the Te–Sb bonds are likely disguised as Te–Te bonds.

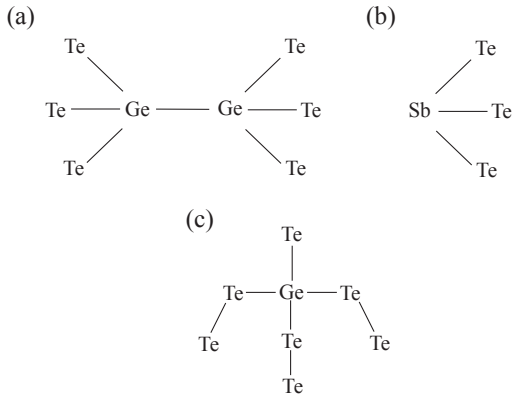

*Fig. 3. Representations of **(a)** Ge_2Te_3 molecular structure, **(b)** Sb_2Te_3 molecular structure, and **(c)** $Ge_{17}Te_{83}$ molecular structure.*

The physical requirement that the number of constraints in an amorphous material equals the number of degrees of freedom in the space that material occupies (or network dimensionality) defines a simple criterion for an ideal, strain-free thin film or bulk material [6]. For the thin film materials addressed in this paper, which are neither i) one-dimensional nor ii) two-dimensional and non-planar networks, the latter bond constraint metric is three, so that the average number of bonds/atom C_{av} is given in Eq. (1),

$$C_{av} = 3. \tag{1}$$

This equation provides the basis for the application of BCT for discriminating between materials with different degrees of ideality in the context of the "ease of glass formation". When it is satisfied, $C_{av} = 3 \pm 0.1$, and a material may be considered to be a "good- glass former." This criterion will be important in identifying the ease of reversible optical or electrical switching in thin film amorphous materials for memory applications.

In proposing this definition for easy glass formation, Phillips [6] underscores the fact that the comparison considers the material from two different perspectives. The $C_{av} \approx 3$ standard represents the number of degrees of freedom/atom in real space, i.e. in a three-dimensional network solid. It also provides a basis for application of simple mechanical models of local or valence forces. It has been shown that C_{av} is related to the average bonding coordination/atom, N_{av}, but should be viewed – from Phillips' other perspective – as the number of constraints in interatomic force field space. The subtlety of BCT comes in determining the number of bonding constraints/atom in any given system. One aspect of this application not included in Refs. 6 or 7, but addressed below relates to broken bonding-bending constraints that derive from certain types of local bonding arrangements

For a system comprised of 2-, 3-, and 4-fold coordinated atoms with N atoms in its molecular formula, C_{av} can be written in terms of the stretching and bending constraints, f_s and f_b, respectively. If n_r is the number of atoms with r-fold coordination in one molecular unit, it

follows that

$$C_{av} = \frac{1}{N}\sum_{r=2}^{4} n_r (f_s + f_b). \quad (2)$$

Each bond represents one stretching constraint, and each is shared by two atoms, thus $f_s = r/2$. In a local three dimensional bonding arrangement the number of bending constraints for an r-fold coordinated atom is $f_b = 2r - 3$ [6], and the following relation is obtained:

$$C_{av} = \frac{1}{N}\sum_{r=2}^{4} n_r \left(\frac{r}{2} + [2r-3]\right). \quad (3)$$

Taking <r> to be the average co-ordination of the material, then

$$\langle r \rangle = \frac{1}{N}\sum_{r=2}^{4} r n_r \quad (4)$$

and thus

$$C_{av} = \frac{5}{2}\langle r \rangle - 3. \quad (5)$$

The condition that a material be a good glass former expressed in Eq. (1) is then equivalent to the condition that the average coordination be given by

$$\langle r \rangle = 2.4. \quad (6)$$

If the 3- or 4-fold coordinated atoms are in planar, rather than in pyramidal or tetragonal arrangements, then the number of bond bending constraints is smaller, and given by $f_b = r - 1$. This is a symmetry driven reduction of restraints that applies independent of the bond-chemistry, whilst the broken constraints addressed later on are driven primarily by bond chemistry.

An alternate approach that arrives at the same conclusion (Eq. 6) is provided by rigidity theory, as developed originally by LaGrange and Clerk Maxwell, and later elaborated upon by Thorpe and co-workers [7]. This approach considers rigidity in systems with 2-, 3- and 4-fold coordinated atoms in a material with local molecular units of N atoms. In calculating the total number of modes of vibration of such a system, they identify modes that require energy (i.e. constraints) and those that do not. The latter are the so-called zero-frequency or *floppy modes*, given the symbol F. F can be expressed as the difference between the total possible number of vibrational modes of the system, $3N$, and the modes determined by constraint counting. Proceeding in this way, F is given by

$$F = 3N - \sum_{r=2}^{4} n_r \left(\frac{r}{2} + [2r-3]\right). \quad (7)$$

The fraction of zero-frequency modes, $f = F/3N$ may then be calculated using Eq. (4), and is given by:

$$f = 2 - \frac{5}{6}\langle r \rangle. \quad (8)$$

With increasing average network coordination, <r>, the fraction of zero frequency modes f decreases, and is exactly equal to zero at the condition given by in Eq. (6). The relationship between f and <r> for <r> = 2.4 is given by the solid line of Fig. 4. The equivalence of the approach based on the assumption inherent in BCT (Eq. (1)) and the approach of rigidity theory (Eq. (6)) is manifest in the fact that each identify a material with <r> = 2.4 as lying at a nexus dividing materials that are floppy form those that are stressed-rigid with respect to material properties.

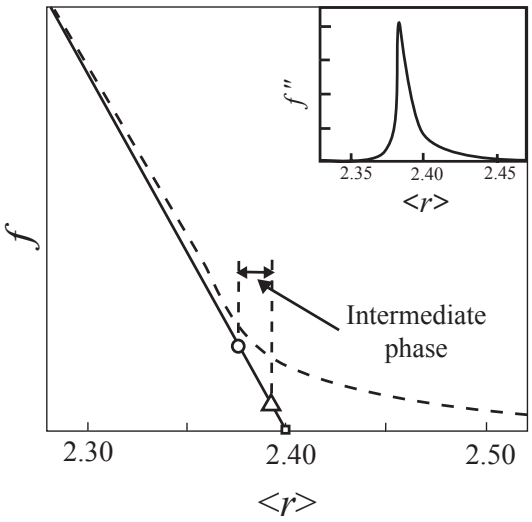

Fig. 4. Plot of f as a function of $\langle r \rangle$. Theory shown by solid line and model shown by dashed line. Inset shows second derivative of f as a function of $\langle r \rangle$. Figure adapted from Ref. 7.

Results obtained by the Thorpe group go beyond the simple analytical treatment outlined above [13]. This research also includes computer modeling of large networks of atoms. Such modeling provides a numerical determination of the fraction of zero-frequency modes, f. Plots of f as a function of <r> reveal three distinct composition regions. One such plot for a system of 2-, 3-, and 4-fold coordinated atoms is shown as the dashed line of Fig. 4. A transition region is readily identified in a plot of the second derivative of f with respect to <r>. This is as shown in the inset of the figure. This plot identifies a narrow transition region, 2.37 < <r> < 2.44, between floppy and stress-rigid regimes. The lower bound of this transition region represents the development of small and isolated pockets of rigid clusters, or *local rigidity*, the number of which increases as the average coordination increases. The upper bound indicates the percolation, or interconnection of, these locally rigid clusters, i.e., *global rigidity*, to generate a stressed-rigid material. For alloys with multiply-coordinated atoms such as $Ge_xSb_yTe_{1-x-y}$ numerical modeling efforts such as this clearly identify three types of material with different values of C_{av}: i) a floppy a material with low average coordination; ii) a stressed-rigid material with high average coordination; and iii) an intermediate-phase material near <r> = 2.4 that is an ideal locally stressed material without percolation of strain, or *unstressed rigid*.

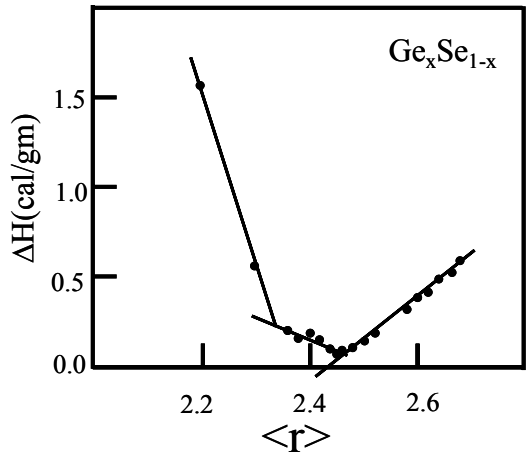

Fig. 5. ΔH as a function of average coordination $\langle r \rangle$ for Ge_xSe_{1-x}. Figure adapted from Ref. 14.

Experimental identification of the three regimes of material appears in several studies by the Boolchand group [14]. One such study presents the heat of formation of Ge_xSe_{1-x} as function of coordination. The data shown in Fig. 5 clearly indicate three distinct regions, with the onset of local rigidity occurring at $\langle r \rangle \approx 2.4$, and the percolation of rigidity at $\langle r \rangle \approx 2.52$. While the data are perhaps not sufficient to define the intermediate unstressed-rigid regions to three significant figures as a function of $\langle r \rangle$, it is clear that the extent of the intermediate phase, $2.4 < \langle r \rangle < 2.52$ is approximately equal to that quite close to those identified in the modeling work of Thorpe, i.e. $2.37 < \langle r \rangle < 2.44$.

Amorphous networks of $Ge_xSb_yTe_{1-x-y}$ are comprised of 2-, 3-, and 4-fold coordinated atoms and are expected to behave much as the materials studied by the Boolchand group and modeled by the Thorpe group. That is, a low coordination floppy material would be expected to allow for *easy* glass formation, but substantial steric freedom would result in a large number of defects in such glasses. As coordination increases the edge of the glass-forming region is approached on a ternary alloy diagram such as Fig. 7, and pockets of rigidity begin to form. At slightly larger coordination, rigidity percolates and the material becomes stressed-rigid. [14] The narrow halo of material compositions lying between these latter two transitions may then be considered to be an intermediate phase, or unstressed-rigid. Materials in this regime are expected to be good glass formers, and additionally may exhibit reversible photo- or electrically- induced switching between amorphous and crystalline phases, provided that the barrier between these phases is low for both the forward and reverse transitions.

In their study of the optical changes accompanying phase transitions in GST alloys, Yamada *et al.* found that the associated change in optical transmissivity is an increasing function of over-coordinated Te [16]. A representation of these data appears as Fig. 6. Abscissa values are determined from simple alloy bond-counting (as done for a-225) while ordinate values can be determined from the published data. Errors on the transmissivity values were estimated from the published plots [16]. No error bars are given for the fraction of over-coordinated Te since these values are numerically determined assuming a continuous random network. The abscissa error bar placed over the point for the a-225 sample reflects the error involved with experimental determination of the fraction of over-coordinate Te based on the EXAFS results. The direct correlation between the magnitude of the switching effect and the fraction of three-fold coordinated Te bonds is instructional. It suggests that these over coordinated Te atoms drive the amorphous-crystalline transition. Furthermore, the dotted straight line in Fig. 6 is reminiscent of a similar trend line found along the composition tie line in the Ge–Sb–Te system, as shown in Fig. 7, along which compositions vary with Te. Obtaining EXAFS data on $Ge_2Sb_2Te_4$ and $Ge_2Sb_2Te_7$ will allow us to understand the local structure of these glass formers and, as a result, study the relationship between over-coordinated Te and phase transitions.

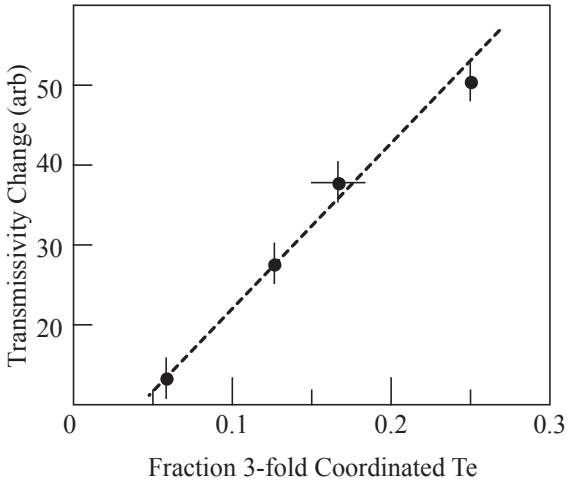

Fig. 6. Transmissivity difference (in arbitrary units) as a function of the fraction of three-fold coordinated Te atoms for amorphous-crystalline transitions in GST alloys. Transmissivity data are from Ref. [16] and three fold coordinated Te atom fraction is deduced from alloy composition.

To calculate where a-225 lies on the ternary phase diagram with respect to the locus of the unstressed rigid material regime, we can view EXAFS data in light of BCT to find the answer. We start by first analyzing the possible vibrational modes in our system. Let us first look at the local bonding environment of Te. Te goes into the system as [A]–Te–[B], where A and B can be Ge, Sb, or Te. We can remove constraints around the Te atom if A and B are different, for instance Ge–Te–Te or Sb–Te–Ge as described before [9]. The bending constraint is retained if A and B are the same.

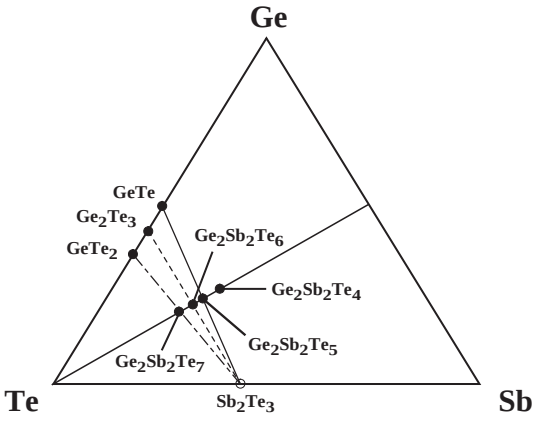

Fig. 7. Compositions of interest, and their theoretical molecular constituents, in the Ge-Sb-Te ternary system along the tie-line of varying Te.

In total, there are 9 possibilities for [A]–Te–[B], if we take into consideration the Ge_2Te_3, $Ge_{17}Te_{83}$, and Sb_2Te_3 molecular structure. Three of these possibilities for A and B, Ge–Te–Ge, Sb–Te–Sb, and, Te–Te–Te, do not allow for constraint removal. For these $1/3$ of the possible Te configurations, the bending constraint is retained and C_{av} = 2. For the remaining $2/3$ of the possible bond configurations around Te, bending constraints can be removed and C_{av} = 1. Hence, the total constraints per Te atom, whilst $Ge_{17}Te_{83}$ is allowed, is

$$C_{av(Te)} = \left(\frac{2}{3}\times 1\right)+\left(\frac{1}{3}\times 2\right)=\frac{4}{3} \qquad (9)$$

In systems where no Te–Te bonds are permitted, only 4 of the [A]–Te–[B] combinations are possible. Of these, a bending constraint can be removed in two of the cases, hence:

$$C_{av(Te)} = \left(\frac{1}{2}\times 1\right)+\left(\frac{1}{2}\times 2\right)=\frac{3}{2} \qquad (10)$$

Assuming no like atom bonding in the Sb_2Te_3 three-fold pyramidal structure, then there are 1.5 stretching constraints and 3 bending constraints, resulting in 4.5 total constraints, none of which are broken.

The EXAFS results in Table 1 give a total coordination for Ge of approximately four. The result is clearly an indication of tetrahedral coordination for all of the Ge atoms. To zeroth order, a tetrahedral Ge configuration yields C_{av} = 7, with five bending and two stretching constraints/atom. However, the inclusion of homopolar Ge-Ge bonds as well as the removal of Te bending constraints have a profound effect on constraint counting.

Table 1. Coordination numbers and nearest neighbor bond distances for a-$Ge_2Sb_2Te_5$ as determined by EXAFS. Internal consistency is manifest in identical values (within the error) for heteropolar bonding distances when using x-ray absorption data from either atomic species.

Table 1. Coordination number and interatomic distances for $Ge_2Sb_2Te_5$.

Atom	Bond	Coordination	R (Å)
Ge	Ge-Te	3.3 ± 0.5	2.63 ± 0.01
	Ge-Ge	0.6 ± 0.2	2.47 ± 0.01
Sb	Sb-Te	2.8 ± 0.5	2.83 ± 0.01
	Sb-Te	*0.5 ± 0.3*	*2.51 ± 0.01*
Te	Te-Ge	1.2 ± 0.3	2.62 ± 0.01
	Te-Sb	1.2 ± 0.3	2.83 ± 0.01

There are two local molecular bonding models to consider, Ge_2Te_3, and $Ge_{17}Te_{83}$, both important for constraint counting. In both cases, there are bending constraints around each Ge atom that are a mixture of Ge-Ge-Te and Te-Ge-Te motions. The force constant for the Ge-Ge-Te bending motion is significantly reduced with respect to that of a Te-Ge-Te bending motion due to the different Ge-Ge-Te and Te-Ge-Te bond energies. In Ge_2Te_3 (not $Ge_{17}Te_{83}$), this permits the removal of 2.67 bending constraints (1.67 from two doubly-degenerate E-mode vibrations and 1 for a non-degenerate A-mode vibration). Thus, the total number of bond-bending constraints around the average Ge atom in this configuration is reduced from 5 to 2.33. With the analysis of the vibrational modes complete, we can now apply BCT to a-225.

In a-225, for simplicity, we assume that there are equal amounts of $Ge_{17}Te_{83}$ and Ge_2Te_3. In cases where the former occurs, 5 of the 9 possible combinations for A and B around Te allows Te–Te bonding and Eq. 9 is required. Thus, we obtain,

$$C_{avTe} = \left(\frac{4}{9}\times 1.5\right)+\left(\frac{5}{9}\times 1.33\right)=1.41 \qquad (11)$$

Of the 11 possible Ge bonds in the system, 7/11 allows us to remove bending constraints, giving:

$$C_{av(Ge)} = \left(\frac{7}{11}\times 4.33\right)+\left(\frac{4}{11}\times 7\right)=5.30 \qquad (12)$$

These results, combined with the constraints removed about Sb, gives:

$$C_{av} = \frac{C_{av(Ge)}\times 2 + C_{av(Sb)}\times 2 + C_{av(Te)}\times 5}{9}$$

$$C_{av} = \frac{5.30\times 2 + 4.50\times 2 + 1.41\times 5}{9} \qquad (13)$$

$$C_{av} = 2.96$$

This value of C_{av} nears the ideal value of 3 suggested for a material in the stress-free state, and more importantly, for a good glass former. Furthermore, from Eq. 9, we see that

$$\langle r \rangle_{effective} = \frac{2}{5}(C_{av} + 3) = 2.38 \qquad (14)$$

This is approximately the ideal value, where $\langle r \rangle \approx 2.4$, where there is ideal local stress in the material without percolation of stress.

4. Conclusions

EXAFS studies on the as-deposited amorphous 225 system are presented. Analysis of the Ge K spectrum shows significant concentrations of both Ge-Ge and Ge-Te bonds. Additionally, concurrent analysis of the EXAFS spectra yields internally self-consistent atomic coordination numbers and bond lengths. Combined with bond-energies for the a-225 system, the EXAFS results show that $Ge_2Sb_2Te_5$ is composed of units of Ge_2Te_3, $Ge_{17}Te_{83}$, and Sb_2Te_3, with i) 17% of the Te atoms 3-fold, rather than 2-fold coordinated, ii) Ge atoms participating in Ge_2Te_3 structures, and iii) Te–Te bonds present in the $Ge_{17}Te_{83}$. These Te–Te bonds are assumed to be "hidden" in the EXAFS as Sb-Te bonds, due to the indistinguishability of Te and Sb. The average atomic coordination, $\langle r \rangle$, and average number of bond-stretching and -bending constraints/atom, C_{av}, has been determined using bond constraint theory for the a-225 system. The inclusion of Ge-Ge bonding and Te bending constraint removal provides the microscopic basis for the good glass forming capability of GST and its propensity for repeatable phase change transitions. The change in overcoordinated Te along the tie line joining the $Ge_2Sb_2Te_4$, $Ge_2Sb_2Te_5$, and $Ge_2Sb_2Te_7$ may be significant to the amorphous-crystalline transition, and will be studied further. EXAFS study and comparison of these alloys will provide us with a new direction for understanding the mechanism of phase change in the Ge-Sb-Te system.

Acknowledgements

Work supported by the Air Force Research laboratory under grant no. F29601-03-01-0229 and by the National Science Foundation under grant no. DMR 0307594. Use of the Advanced Photon Source was supported by the U. S. Department of Energy, Office of Science, Office of Basic Energy Sciences, under Contract No. W-31-109-ENG-38. MRCAT operations are supported by the Department of Energy and the MRCAT member institutions.

References

[1] S. R. Ovshinsky, Phys. Rev. Lett. **20**, 1450 (1968).
[2] C. Peng, M. Mansuripur, Appl. Optics **43**, 4367 (2004).
[3] D. E. Sayers, F. W. Lytle, E. A. Stern, Phys. Rev. B. **11**, 4836 (1975).
[4] A. V. Kolobov, P. Fons, A. I. Frenkel, A. L. Ankudinov, J. Tominaga, T. Uruga, Nature Mater. **3**, 703 (2004).
[5] J. C. Phillips, J. Non-Cryst. Solids **34**, 153 (1979).
[6] M. F. Thorpe, J. Non-Cryst. Solids **57**, 355 (1983).
[7] J. L. LaGrange, Mécanique Analytique, Paris (1788).
[8] J. C. Maxwell, Philos. Mag. **27**, 294-299 (1864).
[9] D. A. Baker, Phys. Rev. Lett. **96**, 255501 (2006).
[10] F. A. Cotton, G. Wilkinson, Advanced Inorganic Chemistry, 3rd Edition (Interscience Publishers, New York, 1972), Chap. 3, p. 117 (Table 3.4).
[11] M. A. Paesler , D. A. Baker, G. Lucovsky, A. E. Edwards , P. C. Taylor, J. Optoelectron. Adv. Mater. 8:6, 2039 – 2043 (2006).
[12] J. P. De Neufville, Chemical aspects of glass formation in telluride system, J. Non-Cryst. Solids **8-10**, 85-105 (1972).
[13] A. Feltz, Amorphe und glasartige anorganische Festkörper, (Akademi-Verlag, Berlin, (1983), p. 248.
[14] R. Kerner, J. C. Phillips, Solid State Communication **117**, 47 (2001).
[15] Xingwei Feng, W. J. Bresser, P. Boolchand, Phys. Rev. Lett. 78, 23 (1997).
[16] Noboru Yamada, Eiji Ohno, Kenichi Nishiuchi, Nobuo Akahira, Masatoshi Takao, J. Appl. Phys. **69**, 2849 (1991).

*Corresponding author: Paesler@ncsu.edu